Journal of Hazardous Materials 397 (2020) 122746

Contents lists available at ScienceDirect

Journal of Hazardous Materials

journal homepage: www.elsevier.com/locate/jhazmat

Transcriptome analysis of the effect of bisphenol A exposure on the growth, photosynthetic activity and risk of microcystin-LR release by Microcystis aeruginosa

Meng Yang, Zhengqiu Fan, Yujing Xie, Lei Fang, Xiangrong Wang*, Yuan Yuan, Rongxi Li

Department of Environmental Science and Engineering, Fudan University, Shanghai 200438, China

GRAPHICAL ABSTRACT

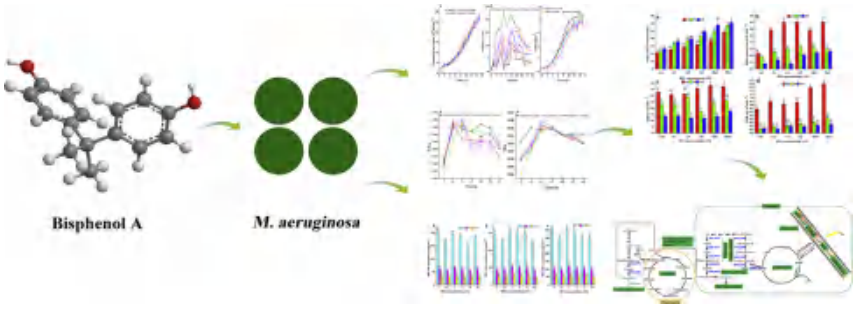

ARTICLE INFO

R. Debora

Keywords:
BPA toxicity
Photosynthesis
Microcystins
Oxidative stress
Transcriptomics

ABSTRACT

Bisphenol A (BPA), one of the most abundant endocrine-disrupting compounds, is frequently detected in diverse aquatic environments, which imposes a substantial burden on the aquatic ecosystem. However, the correlation between BPA levels and the outbreak of a cyanobacterial bloom remains largely unknown. In this study, the cellular and transcriptomic responses to BPA exposure were investigated. Exposure to a high concentration of BPA (50 μM) significantly inhibited the growth of cyanobacterial cells, with the highest inhibition ratio of 51.3%, photosynthesis, and the release of extracellular microcystin-LR (MC-LR) ($p < 0.05$). However, exposure to low concentrations of BPA (0.1 and 1 μM) also affected these indicators, but the differences were closely related to the growth phase of the cyanobacterial cells. In addition, an imbalance between the antioxidant system and oxidative stress was observed in cyanobacteria under BPA stress. Folate biosynthesis, ABC transporters and ubiquinone and other terpenoid-quinone biosynthesis were the central metabolic pathways triggered by BPA stress. The up-regulated genes, including queC, VTE3 and PsbO were the controller of cellular growth and photosynthesis. The down-regulated genes, including VET4, MlaE and DnaA were potential biomarkers of oxidative damage. The up- and down-regulated genes, including CA, Ppc and CyoE were the main regulators of energy generation. The findings will provide important insights into the role of endocrine disruptors in the frequent outbreak of cyanobacterial blooms.

* Corresponding author.
E-mail address: xrxrwang@fudan.edu.cn (X. Wang).

https://doi.org/10.1016/j.jhazmat.2020.122746
Received 22 December 2019; Received in revised form 7 March 2020; Accepted 13 April 2020
Available online 29 April 2020

1. Introduction

Bisphenol A (BPA) is widely applied to various products that affect all aspects of people's daily lives, such as epoxy resins, polycarbonate plastics, food and beverages cans, dental composites/sealants, dish and laundry detergents and care products (Fenichel et al., 2013; Fleisch et al., 2010; Dodson et al., 2012). Its high production volume, incomplete removal during wastewater treatment and leaching from the discharge of BPA-containing consumer products, leads to the frequent detection of BPA in the natural environment (Robinson et al., 2009; Melcer and Klecka, 2011; Sajiki and Yonekubo, 2003). A BPA concentration of 174.6 ng mL^{-1} was detected in the microbasin of the Apatlaco River by Ronderos-Lara et al. (2018). In surface water, a BPA concentration of 56 μg L^{-1} was reported by Corrales et al. (2015). Due to the increasing demand for BPA-based products, BPA pollution in the natural environment will become increasingly serious (Huang et al., 2012). According to a recent survey, BPA has been detected at a high frequency (up to 99%) in human urine samples (Ye et al., 2015). Because of the health concerns associated with BPA exposure (Sekizawa, 2008; Hengstler et al., 2011; Shelby, 2008), additional studies of the fate and effect of BPA on the natural environment are required. Currently, some evidence supports the hypothesis that cyanobacterial blooms serve as the sink and source of endocrine disruptors in freshwater lakes in China (Jia et al., 2019); however, no data exist to elucidate the real role of endocrine disruptors in the frequent outbreak of cyanobacterial blooms.

Recently, some studies described the effects of BPA on algae, which mainly focused on the changes in the algal growth dynamics induced by BPA. The addition of BPA was detrimental to the algae growth, but the effect was weakened as the nitrogen or phosphorus concentration increased (Yang and Wang, 2019a, b). These emerging studies have substantially improved our understanding of the role of BPA in algae growth; however, the ecological risks of BPA are not completely understood. In addition, these studies were mainly conducted when phytoplankton reached their logarithmic growth stage, during which phytoplankton usually exhibit the best metabolic activities and are able to resist external disturbances. Therefore, the published literature may underestimate the adverse effects of BPA on phytoplankton growth. To our knowledge, limited information is available about the physiological effects of BPA on freshwater algae throughout the growth cycle, but these data are essential for understanding the true role of BPA.

Hence, one of the toxin-producing cyanobacterial harmful algal blooms genera in freshwater ecosystems, Microcystis aeruginosa was used as a representative of prokaryotic algae to examine two aspects of the possible regulatory effect of BPA on M. aeruginosa in this study. First, M. aeruginosa were exposed to BPA levels reaching or exceeding the upper limit of environmentally relevant concentrations, which ranged from 0.1 − 50 μM, and then the optical density (OD_{680}), population growth inhibition, chlorophyll a (Chl-a) content, chlorophyll a fluorescence, antioxidant responses, reactive oxygen species (ROS) and lipid peroxidation levels and the risk of MC-LR release from M. aeruginosa were measured during the 15-d period. Secondly, the transcriptome-based analysis of gene expression of M. aeruginosa was performed to provide insights into the regulatory mechanism of BPA at the molecular level. The aim of this study is to obtain comprehensive insights into the regulatory mechanism of BPA on cyanobacteria during long-term exposure. The observations will provide important clues to evaluate the physiological and molecular effects of endocrine disruptors on the frequent outbreak of cyanobacterial blooms.

2. Materials and methods

2.1. Strains and reagents

The strain M. aeruginosa FACHB905 was supplied by the Freshwater Algae Culture Collection at the Institute of Hydrobiology (FACHB-Collection, Wuhan, China). Bisphenol A (BPA) was purchased from Sigma-Aldrich (St. Louis, MO, USA).

2.2. Microbial culture and bisphenol A treatment

M. aeruginosa were cultured at 25 ℃ with a light-dark cycle of 12: 12 h (4000 lx). At the exponential growth phase, cells were harvested, centrifuged, and then re-suspended to prepare the cyanobacterial suspensions at an initial density of 1.87 (± 0.02) × 10^6 cells mL^{-1} in a 1000 mL Erlenmeyer flask. Subsequently, a stock solution of BPA at 1.0 g L^{-1} was diluted to the different test concentrations to add into the BG11 medium to gain the following final nominal concentrations: 0 (control), 0.1, 1, 5, 10 and 50 μM. Each treatment has three biological replicates.

2.3. Cyanobacterial growth

Cultures of M. aeruginosa were aseptically sampled daily until day 15, to measure the cell density by recording the optical density at a wavelength of 680 nm (OD_{680}). A standard curve showing the cell density as a function of OD_{680} was generated from a standardized cyanobacteria culture and a hemocytometer. The following regression equation was used, y indicates the cell counts, × 10^6 cells mL^{-1}, and x was the optical density of 680 nm (OD_{680}): y = 12.054 × −0.0543 (R^2 = 0.9961). The growth inhibition rate (IR) was calculated using Eq. (1):

$$IR = \left(1 - \frac{C}{C_0}\right) \times 100\% \quad (1)$$

where C is the cell count of treated group, C_0 is the cell count of the control group. The Chl-a content was determined according to our previous published method (Yang and Wang, 2019b).

2.4. Chlorophyll *fl*uorescence analysis

Cyanobacterial cells in each test group were collected every 2 d to analyze the chlorophyll fluorescence. A series of photosynthetic activity parameters, including the maximum and actual photochemical quantum yield of photosystem II (PSII) (F_v/F_m and Φ_{PSII}), rapid light curve (RLC), the maximum potential relative electron transfer rate without photoinhibition (rETRmax), the initial slope (α), the semi-light saturation point (I_k) and the non-photochemical quenching (NPQ), were determined using a PhytoPAM fluorescence monitoring system (Walz, Germany). The maximum and actual photochemical quantum yield of photosystem II (PSII) (F_v/F_m and Φ_{PSII}) were calculated using Eqs. (2) and (3), respectively:

$$\frac{F_v}{F_m} = \frac{F_m - F_0}{F_m} \quad (2)$$

$$\Phi_{PSII} = \frac{\Delta F}{F_m'} = \frac{Fm' - F_s}{F_m'} \quad (3)$$

where F_0, F_m, F_s and F_m' are the minimum and maximum fluorescence, the light-acclimated steady-state fluorescence, and maximum fluorescence (F_m'), respectively.

The relative electron transport rate (rETRmax), which is associated with the overall photosynthetic performance of microalgae, was determined by fitting a curve of rETR versus PAR, using the equation reported by Platt et al. (1980).

2.5. Determination of the intracellular and extracellular MC-LR

On the third, ninth and fifteenth days of a 15-day exposure period, 20 mL of culture were harvested by centrifugation at 10,000 rpm for 10 min at 4 ℃, and the supernatant was filtered with a 13 mm diameter nylon syringe filter (0.22 μm pore size) to obtain the solution containing the extracellular MC-LR (Fraction A). Thereafter, the centrifugal

sediment was thoroughly dissolved in 5 mL of 50% methanol/water (v/v) containing 1% acetic acid (v/v) in an ultrasonic cell homogenizer on ice for 5 min at 350 W (Boyer, 2007). Subsequently, the homogenate was then centrifuged at 12,000 rpm for 10 min at 4 °C to produce the supernatant and eventually obtain the intracellular MC-LR (Fraction B). Both fractions were measured using a microcystin enzyme-linked immunosorbent assay (ELISA) kit according to the manufacturer's instructions (Chen et al., 2010)

2.6. Determination of intracellular ROS levels, lipid peroxidation and antioxidant capacity

The ROS level analyzed in this study specifically refers to the intracellular ROS level. The cyanobacterial cells were collected on the third, ninth and fifteenth days of exposure. The harvested cyanobacterial cells were used to analyze ROS levels, the malondialdehyde (MDA) content, glutathione (GSH) content, and activity of the antioxidant enzyme superoxide dismutase (SOD). Detailed descriptions of the methods used to measure these indices are provided in Text S1.

2.7. RNA extraction and transcriptomic analysis

The cyanobacterial cells treated with 0.1 and 50 μM of BPA or the control for 15 d were collected for RNA extraction. Detailed descriptions of the methods used to extract the RNA and perform the transcriptomic analysis are provided in Text S2.

2.8. Statistical analyses

Results are presented as means ± standard deviations. Two-way ANOVA was performed to elucidate the effect of the interaction between BPA and exposure time on the cellular eco-physiological indices using SPSS version 23.0 and Duncan's post hoc test ($p < 0.05$). One-way ANOVA was used to compare variable means.

3. Results and discussion

3.1. Effect of BPA on cyanobacterial cells growth characteristics

Analyses of the growth curve and inhibition rate were performed to examine the effect of BPA on the growth of M. aeruginosa (Fig. 1). A significant inhibitory effect on the cyanobacterial cell growth was observed at each BPA treatment, while an inconsistent change in the growth of M. aeruginosa was discovered at different BPA exposure times and concentrations (Fig. 1a). Specifically, before 7 d exposure, the growth of M. aeruginosa treated with 10 and 50 μM BPA was significantly restrained ($p < 0.05$). After BPA exposure of 7 d, the cyanobacterial cells counts in the BPA treatment groups were all significantly lower than the control group ($p < 0.05$). Meanwhile, the inhibition of cyanobacterial cell growth was more significant as the concentrations of BPA increased. Compared to the control, BPA concentrations of 1−50 μM produced growth inhibition rates of 10.9%, 15.4%, 15.9% and 21.8%, respectively, after 15 d of exposure (Fig. 1b). BPA concentrations of 0.099, 0.014, and 0.317 μg L^{-1} were detected in drinking (tap) water from North America, Europe and Asia, respectively, by Arnold et al., (2013). In some water and effluent, BPA levels of 0.01 μg L^{-1} to 17.2 mg L^{-1} were reported by Michalowicz (2014). In freshwaters samples, the effective concentration of BPA of 9.663 ± 0.047 mg L^{-1}, which triggered a 50% inhibition of the growth of C. raciborskii, was observed by Xiang et al. (Xiang et al., 2018a). Therefore, concentrations of 0, 0.1, 1, 5, 10, 50 μM were used in this study, because they are close to environmentally relevant concentrations in natural waters. The growth inhibition rates observed in this study suggested that the growth of M. aeruginosa was altered by BPA at environmentally relevant concentrations. The possible interpretation was that higher BPA concentrations might disrupt cell division, folding modification pathways and signaling pathways, resulting in the cracking and disintegration of the cell structure. The alterations in the Chl-a levels of M. aeruginosa treated with different BPA concentrations are shown in Fig. 1c. Chl-a accumulated throughout the culture period. Under BPA stress, Chl-a synthesis was significantly inhibited. Moreover, more significant inhibition of Chl-a synthesis was observed in the presence of higher BPA concentrations. At a concentration of 50 μM, BPA significantly inhibited Chl-a synthesis throughout the exposure period ($p < 0.05$), and the highest inhibition rate was 51.3%. A similar finding was reported by Xiang et al. (2018b) When Cylindrospermopsis raciborskii was exposed to BPA, the mechanism by which BPA inhibit photosynthesis was that BPA blocked the electron transfer of PSII from plastoquinone to the quinone pool.

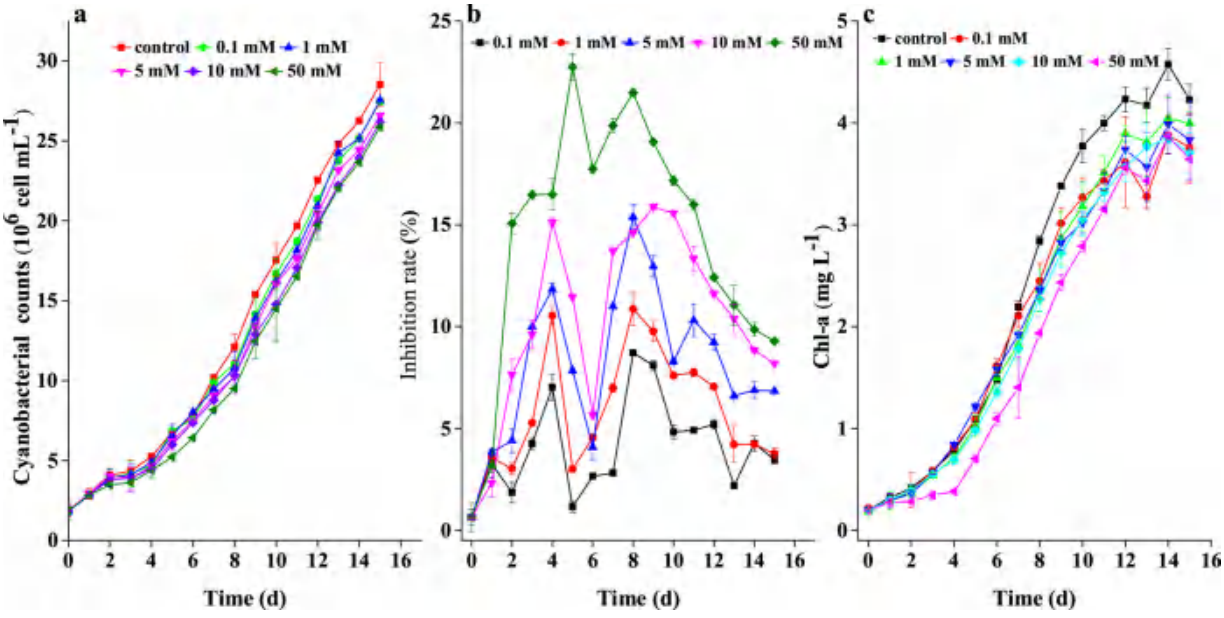

Fig. 1. Growth characteristics of M. aeruginosa during 15 d cultivations. (a) Cyanobacterial cells counts; (b) cyanobacterial cells growth inhibition rate (IR); (c) Chl-a, chlorophyll a content in response to different concentration of BPA (Mean and standard deviation of three replicates are shown).

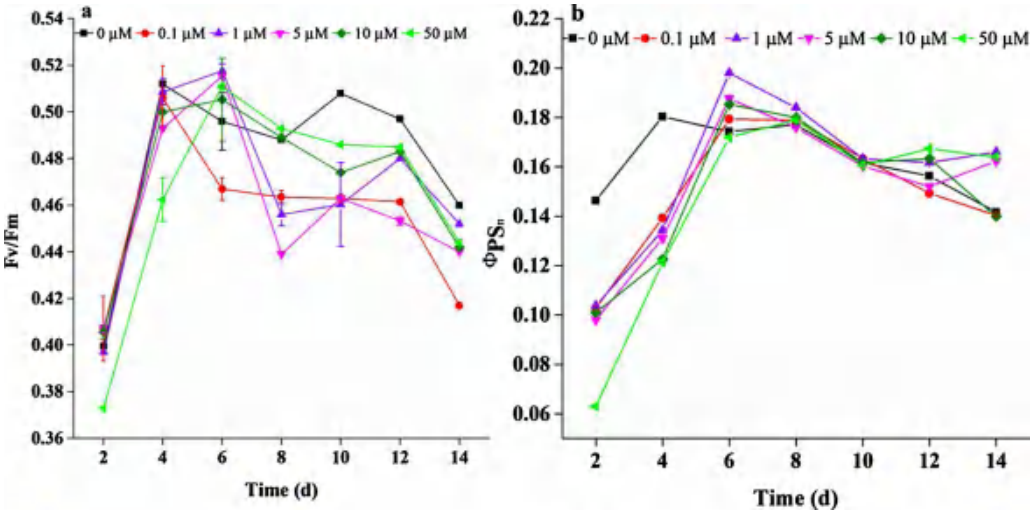

Fig. 2. Effects of BPA on (a) the Fv/F_m value and (b) the Φ_{PSII}value in M. aeruginosa during 15-d cultivation. Data shown are mean values ± standard deviation. Error bars indicate standard deviation (n = 3).

3.2. Effect of BPA on the photosynthetic performance of cyanobacterial cells

The photosynthetic efficiency parameters (F_v/F_m, Φ_{PSII}) were substantially altered by BPA after 15 d of cultivation. F_v/F_m initially exhibited an increasing trend, followed by a decreasing trend during the cultivation period (Fig. 2a). F_v/F_m is an important indicator of the effects of photoinhibition or various environmental stresses on photosynthesis (Ng et al., 2014). Φ_{PSII} initially increased and then decreased (Fig. 2b). Based on these results, BPA reduced the maximum and actual photochemical efficiency of PSII. Moreover, more significant inhibition of F_v/F_m was observed in cells exposed to higher concentrations of BPA, indicating that higher concentrations of BPA exerted a stronger inhibitory effect on photosynthesis in M. aeruginosa. At the same time, the electron transport rate, the solar energy utilization efficiency and tolerance ability to strong light of M. aeruginosa were restrained by exposure to a high BPA concentration, as revealed by the decreasing trends for four photosynthesis parameters: ETRmax, alpha, Ik and NPQ (Fig. 3). Additionally, the NPQ value indicates the microalgal photosynthetic protection mechanism (Markou et al., 2017). However, the microalgal protection mechanism functioned only for approximately 2 d, and then the NPQ value gradually decreased to approximately zero, implying the collapse of the microalgal photosystem (Fig. 3d).

The growth phase of cyanobacterial cells also exerts a substantial effect on their photosynthesis. The activity in aging cultures and light availability may become limiting factors as the algal cell biomass increases, resulting in changes in photosynthetic parameters (Oukarroum, 2016). This evidence for this phenomenon in the present study was the increasing Chl-a content and decreasing NPQ value, which implied that the photosynthesis in M. aeruginosa is impaired at the late growth stage.

3.3. Effect of BPA on intracellular and extracellular MC-LR levels

Intracellular, extracellular and total MC-LR levels were calculated as the value of the cell quota. As shown in Fig. 4, cells in the lag growth phase showed a higher mean microcystin quota than cells in the exponential and stationary phases, suggesting that the growth phase of algal cells was a limiting factor affecting the production and release of MC (Table 1). A similar finding was reported in the study by Wu et al. (2015), as the M. aeruginosa biomass increased rapidly and the rate of MC-LR production was lower than cell division during the exponential growth phase, which might be responsible for the decrease in the MC-LR content per cell over the entire exposure period in the present study. The lower MC quota observed during the stationary phase might have been due to the higher cell density, which was confirmed by the highest counts of cyanobacterial cells observed during the stationary growth phase in M. aeruginosa (Fig. 1a).

Both intracellular and extracellular MC-LR levels decreased until the concentration of BPA exceeded 0.1 μM, and then a sharp increase in the extracellular MC-LR level occurred, while the intracellular MC-LR level exhibited a corresponding decrease with increasing BPA concentrations (Fig. 4a). This phenomenon revealed substantial damage to the cyanobacterial cells, and thus a large amount of MC-LR was released into the aquatic environment and the intracellular MC-LR level decreased accordingly. These findings may result from the critical lysis of cyanobacterial cells triggered by BPA stress, resulting in the mutual transfer of MC-LR between the intracellular and extracellular compartments. Further support for this phenomenon was provided in the study by Daly et al. (2007).

3.4. Intracellular ROS levels, lipid peroxidation and antioxidant capacity

ROS levels were significantly increased in cyanobacterial cells exposed to BPA during each growth phase ($p < 0.05$) (Fig. 5a). Additionally, cyanobacterial cells in stationary growth phase from the control and BPA treatment groups produced more ROS than cells in the lag or exponential growth phase. The MDA content was also significantly increased by BPA exposure in cells in each growth phase ($p < 0.05$). Meanwhile, the MDA content was significantly reduced as the culture time increased ($p < 0.05$) (Fig. 5b).

The effects of BPA on the antioxidant capacities (SOD and GSH) of M. aeruginosa are shown in Fig. 5c and d. The SOD activity was not significantly different between the control group and groups treated with low levels of BPA treatment (0.1–1.0 μM) in each growth phase ($p > 0.05$) (Fig. 5c). However, exposure to higher concentrations of BPA (5 − 50 μM) significantly increased the SOD activity by 7.7%, 13.7% and 12.0%, respectively (Fig. 5c). The GSH content was significantly increased by the higher BPA concentrations throughout the growth phase ($p < 0.05$). BPA and the exposure time altered the GSH content in a similar manner to the SOD activity ($p < 0.05$) (Table 1 and Fig. 5d). The GSH content was markedly increased as the BPA concentration increased during each growth phase, and was significantly decreased by the late growth phase under each treatment condition ($p < 0.05$).

The intracellular ROS level increased as the exposure time and concentration of BPA increased (Fig. 5a). This finding implied substantial damage to the antioxidant system of M. aeruginosa and triggered oxidative stress in the cyanobacterial cells. Further evidence for this damage was supplied by the MDA levels. MDA levels are used to

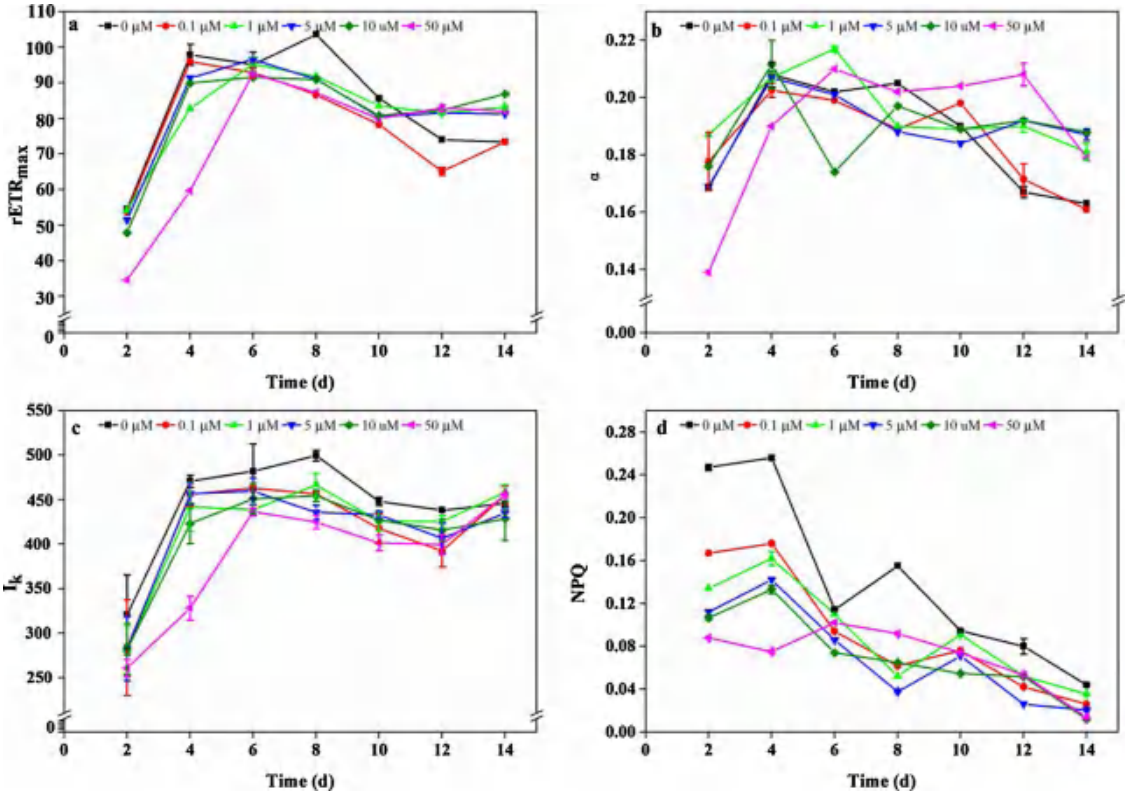

Fig. 3. Effect of BPA on photosynthetic parameters of M. aeruginosa during 15-d cultivation: (a) rETRmax, maximal electron transport rate, (b) α, the initial slope, (c) I_k, the semi-light saturation point, (d) NPQ, non-photochemical quenching. Mean and standard deviation of three replicates are shown.

evaluate the level of cell membrane lipid peroxidation triggered by external environmental stresses (Yang and Miao, 2010). In the present study, a high concentration of BPA induced substantial membrane lipid peroxidation and membrane damage in cyanobacterial cells, consistent with the dose-dependent increase in MDA levels (Fig. 5b). A similar phenomenon was also triggered by other stresses, such as antibiotics (Liu et al., 2015), pesticides (Lu et al., 2018), and nanoparticles (Zhang et al., 2018). However, a significant decrease in the MDA content was observed in the exponential and stationary growth phases, suggesting that less membrane damage occurred in M. aeruginosa that was potentially due to the increased accumulation of the cyanobacterial cell biomass (Xie et al., 2011).

The antioxidant enzyme SOD represents the first barriers in the intracellular antioxidant system that scavenges reactive oxygen species to protect cells from external stress (Blokhina et al., 2003). Many studies have verified that the activities of most antioxidant enzyme, including SOD, CAT and POD, increase in response to exposure to exogenous pollutants (Qian et al., 2008; Liu et al., 2012). Similar to these previous reports, the present study revealed a significant increase in SOD activity in M. aeruginosa exposed to a high BPA concentration (Fig. 5c). Meanwhile, the GSH content was also significantly increased in cells exposed to high BPA concentrations (Fig. 5d). The increased SOD activity may result from the activation of existing enzyme pools or the increased expression of genes that encode SOD, leading to the overproduction of superoxide (Xie et al., 2011; Foyer et al., 1997). The increase in the GSH content was considered an adaptive trait to protect

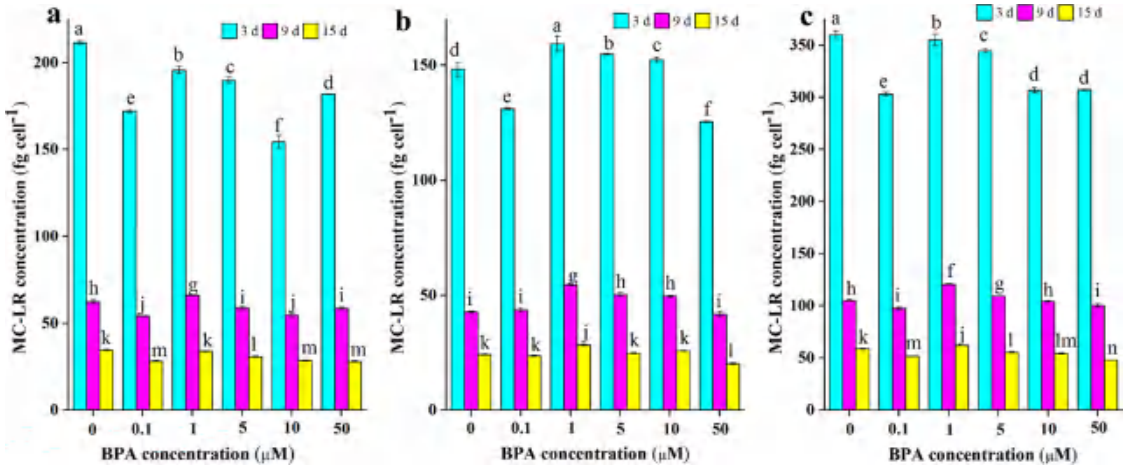

Fig. 4. MC-LR concentration of control and BPA treated samples during 15-d cultivation: (a) intracellular MC-LR, (b) extracellular MC-LR and (c) total MC-LR. Mean and standard deviation of three replicates are shown; different alphabet letters indicate significant difference in means among groups at each BPA level at $p < 0.05$ according to one-way ANOVA test.

Table 1
Summary of two-way ANOVA analysis between the effects of BPA and growth phase on the various cellular contents of M. aeruginosa.

Dependent variables	Factors	DF	F	p
Cyanobacterial cell density	BPA	5	315.536	$p < 0.001$
	GP	2	76159.985	$p < 0.001$
	BPA × GP	10	39.156	$p < 0.001$
Chlorophyll-a content	BPA	5	1062.461	$p < 0.001$
	GP	2	166738.689	$p < 0.001$
	BPA × GP	10	202.047	$p < 0.001$
Intracellular MC-LR	BPA	5	464.782	$p < 0.001$
	GP	2	81845.564	$p < 0.001$
	BPA × GP	10	195.700	$p < 0.001$
Extracellular MC-LR	BPA	5	298.497	$p < 0.001$
	GP	2	51491.226	$p < 0.001$
	BPA × GP	10	82.478	$p < 0.001$
Total MC-LR	BPA	5	380.283	$p < 0.001$
	GP	2	104764.26	$p < 0.001$
	BPA × GP	10	134.017	$p < 0.001$
ROS	BPA	5	8505.559	$p < 0.001$
	GP	2	85469.795	$p < 0.001$
	BPA × GP	10	2426.141	$p < 0.001$
MDA	BPA	5	226.037	$p < 0.001$
	GP	2	146.036	$p < 0.001$
	BPA × GP	10	4.106	$p < 0.001$
SOD	BPA	5	12.74	$p < 0.001$
	GP	2	698.093	$p < 0.001$
	BPA × GP	10	9.523	$p < 0.001$
GSH	BPA	5	236.741	$p < 0.001$
	GP	2	4626.669	$p < 0.001$
	BPA × GP	10	63.656	$p < 0.001$

Abbreviation: Growth phase (GP).

against the damage caused by oxidative stress (Gonçalves-Soares et al., 2012). However, the increasing ROS level and MDA content suggested an imbalance in antioxidant systems, as revealed by the inadequate levels of the antioxidants SOD and GSH (Fig. 5). Therefore, the intracellular over-accumulation of ROS altered membrane permeability, triggered oxidative damage to biomolecules, and generated lipid peroxidation-related signaling molecules, leading to cell dysfunction and death (Mittler, 2002).

3.5. Effect of BPA on global transcriptional changes in M. aeruginosa

The global transcriptomic alterations in M. aeruginosa exposed to 0.1 μM and 50 μM BPA for 15 d were investigated and compared with the control group to further examine the effect of BPA exposure on the expression of functional genes in M. aeruginosa at the molecular level, The expression levels of 43 genes were up-regulated and 58 were down-regulated in the high BPA treatment group (50 μM BPA compared with the control, H/CK), while 40 were up-regulated and 12 were down-regulated in the low BPA treatment group (0.1 μM BPA compared with the control, L/CK) among the 5314 identified proteins (> 2-fold change, $p < 0.05$). These genes are plotted in Fig. S1, and represented the most creditable BPA-regulated genes involved in stimulus response and the altered metabolic network. A Gene Ontology (GO) enrichment analysis of the differentially expressed genes in high and low BPA treatment groups was performed, and the results are shown in Fig. S2. The cellular component analysis in the high BPA treatment group revealed that most of the genes with altered expression were associated with external encapsulating structure, cell wall and cell periphery, while genes in the low BPA treatment group were related to thylakoid membrane and photosynthetic membrane. The differentially expressed genes in the high BPA treatment group have notable molecular functions, including double-stranded RNA-specific ribonuclease activity, dihydroorotate dehydrogenase activity, oxidoreductase activity, acting on the CH-CH group of donors, quinone or related compound as acceptor, phospholipid binding and endoribonuclease activity, while genes in the low BPA treatment group were involved in 2-C-methyl-D-erythritol 4-phosphate cytidylyltransferase activity, pyrimidine

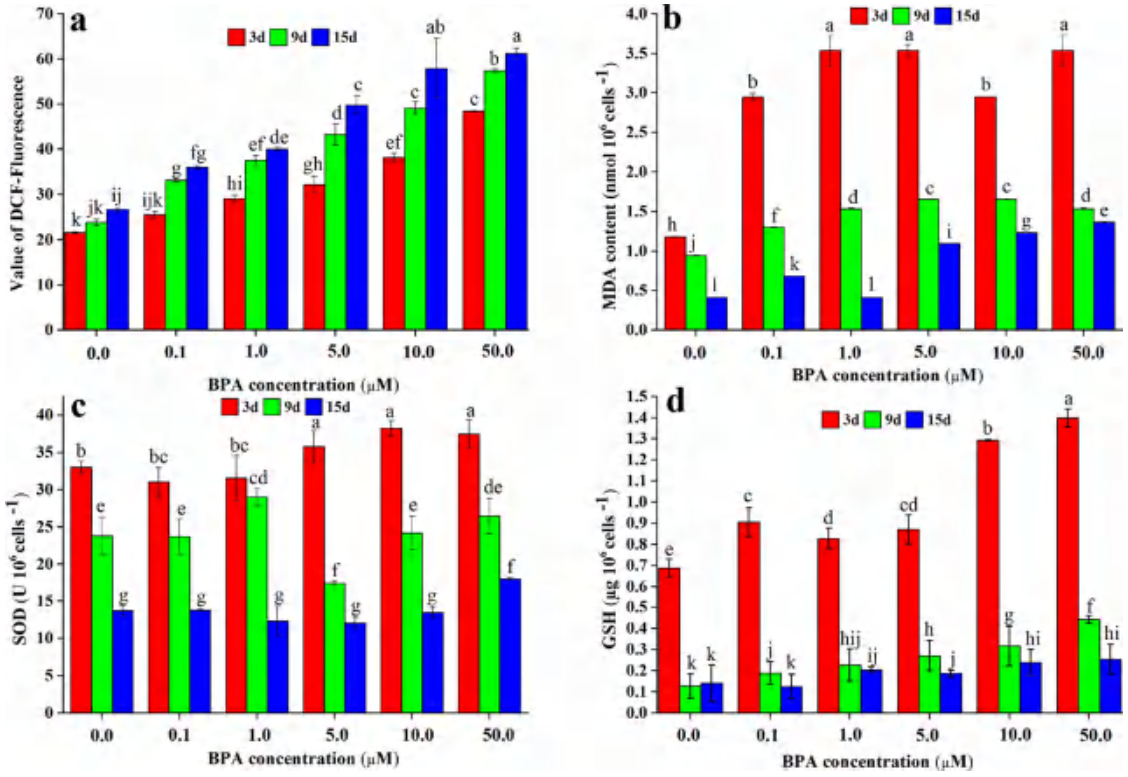

Fig. 5. Effect of BPA on (a) ROS content, (b) MDA content, (c) SOD activity and (d) GSH content of M. aeruginosa at the third, ninth and 15th day of a 15-day exposure period. Mean and standard deviation of three replicates are shown. Different alphabet letters indicate significant difference in means among groups at each BPA level at $p < 0.05$ according to one-way ANOVA test.

Table 2
Potential candidate genes related to the response to BPA stress.

MAE_Number	Gene symbol	Annotation	p value	Fold change	
				L/CK	H/CK
Ubiquinone and other terpenoid-quinone biosynthesis					
00130	BH695_RS16970	Methyltransferase domain-containing protein	$1.15–10^{-271}$	3.23	0.42
00130	BH695_RS16810	Methyltransferase domain-containing protein	$2.61–10^{-19}$	−0.29	−1.07
Folate biosynthesis					
00790	queC	1,7-cyano-7-deazaguanine synthase QueC	$2.94–10^{-11}$	1.62	2.14
00790	BH695_RS05840	1,6-carboxytetrahydropterin synthase	$3.41–10^{-11}$	−1.27	−1.00
Terpenoid backbone biosynthesis					
00900	BH695_RS11500	2-C-methyl-D-erythritol 4-phosphate cytidylyltransferase	$3.21–10^{-5}$	1.03	0.22
ABC transporters					
002010	BH695_RS20280	Iron uptake protein A1	$1.65–10^{-30}$	2.26	0.43
002010	BH695_RS02625	MlaE family lipid ABC transporter permease subunit	$1.55–10^{-18}$	−0.51	−1.00
Glycolysis/Gluconeogenesis					
0010	pckA	Phosphoenolpyruvate carboxykinase (ATP)	$1.02–10^{-16}$	−0.43	−1.04
Citrate cycle (TCA cycle)					
0020	pckA	Phosphoenolpyruvate carboxykinase (ATP)	$1.02–10^{-16}$	−0.43	−1.04
Oxidative phosphorylation					
00190	BH695_RS23775	ProtohemeIX farnesyltransferase	1.46×10^{-14}	−0.28	−1.27
Photosynthesis					
00195	BH695_RS17615	Photosystem II manganese-stabilizing polypeptide	$2.04–10^{-1}$	0.32	1.00
Porphyrin and chlorophyll metabolism					
00860	acsF	Magnesium-protoporphyrin IX monomethyl ester (oxidative) cyclase	$1.02–10^{-1}$	0.80	1.20
00860	BH695_RS23775	Protoheme IX farnesyltransferase	$1.46–10^{-14}$	−0.28	−1.27
Nitrogen metabolism					
00910	BH695_RS03765	Carbonic anhydrase	$2.88–10^{-6}$	0.52	1.13
Two-component system					
002020	BH695_RS10765	Fatty acid desaturase	$1.62–10^{-25}$	−0.45	−1.08
002020	BH695_RS23780	Chromosomal replication initiator protein DnaA	$4.2–10^{-28}$	−0.39	−1.11
Ribosome					
003010	BH695_RS16295	50S ribosomal protein L7/L12	$3.81–10^{-11}$	0.64	1.01
003010	BH695_RS16300	50S ribosomal protein L10	$7.50–10^{-1}$	0.63	1.03
Cell cycle-Caulobacter					
004112	BH695_RS23780	Chromosomal replication initiator protein DnaA	$4.20–10^{-28}$	−0.39	−1.11

nucleoside binding and CTP binding. The biological process analysis indicated that the 101 and 98 genes with altered expression in the high and low BPA treatment groups, respectively, were related to cellular process, growth, localization, metabolic process and response to stimulus (Fig. S2).

A KEGG (Kyoto Encyclopedia of Genes and Genomes) pathway analysis was performed to elucidate the metabolic pathways in which these altered genes are involved in. Based on the results (Table 2), the 101 and 52 genes with altered expression in the high and low BPA treatment groups, respectively, were related to different metabolic pathways in M. aeruginosa ($p < 0.05$) and were mainly involved in ubiquinone and other terpenoid-quinone biosynthesis, folate biosynthesis, terpenoid backbone biosynthesis, photosynthesis, ABC transporters, glycolysis/gluconeogenesis, citrate cycle, oxidative phosphorylation, porphyrin and chlorophyll metabolism, nitrogen metabolism and cell cycle-caulobacter. Furthermore, the KEGG pathway analysis was also utilized to better elucidate the distribution of up- and down-regulated genes. The results revealed that down-regulated genes controlled the most metabolic pathways in high BPA-treated groups, while in low BPA-treated groups, up-regulated genes governed the majority of metabolic pathways (Fig. 6). Folate biosynthesis was significantly enriched in both high and low BPA-treatment groups with enrichment scores of 2.04 and 3.92, respectively, an indication that the cyanobacterial cells were accelerated queuosine production for aggregate formation and promoting their fitness in response to external stress, as evidenced by the up-regulated gene queC (Table 2 and Fig. 6). In high BPA-treated groups, the up-regulated genes were frequently involved in porphyrin and chlorophyll metabolism, ribosome, photosynthesis, nitrogen metabolism. The down-regulated genes in high BPA-treated groups were involved in central carbon metabolism, which includes the pathways of glycolysis/gluconeogenesis, citrate cycle and pyruvate metabolism. Moreover, the altered expressed genes associated with the

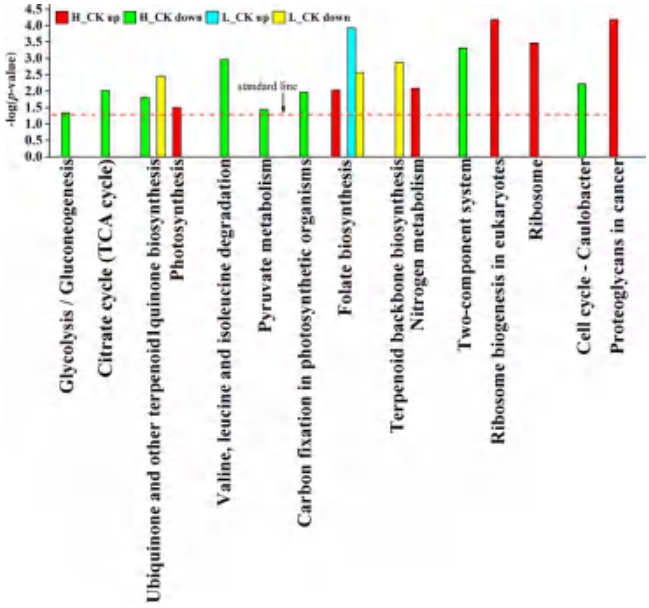

Fig. 6. Pathways associated with up- and down-regulated genes between the post-exposure BG11 with BPA group at 0, 0.1 and 50 μM of BPA and pre-exposure BG11 group were determined using a DAVID analysis. An enhanced score [− log(p value)] of ≥1.3 threshold (red dotted line) was considered significant. (For interpretation of the references to color in this figure legend, the reader is referred to the web version of this article.)

energy metabolism, including oxidative phosphorylation and carbon fixation in photosynthetic organisms, were also down-regulated upon exposure to high BPA concentrations. As the cells were exposed to the

low concentration of BPA, the altered genes were mainly related to the metabolism of cofactors and vitamins, membrane transport and terpenoid backbone biosynthesis, which was responsible for preparing matrix substances for electron transfer and substance metabolism.

3.6. Analysis of alterations in the molecular regulatory network in response to BPA stress

The reaction of splitting water to release oxygen and electrons on the oxygen-evolving complex of photosystem II was continuous, as evidenced by the up-regulation of the gene encoding photosystem II oxygen-evolving enhancer protein 1 (PsbO) to stabilize manganese in photosystem II in high BPA-treated groups. Nonetheless, the capacities of scavenging lipid peroxyl radicals at lipoproteins and cell membranes were substantially affected, as evidenced by the down-regulation of gamma-tocopherol methyltransferase (VET4) in response to high BPA exposure, which may provide a good explanation for the increasing ROS value and MDA content (Fig. 5a and b). However, the plastoquinone that diffuses between photosystem II and Cyt b6/f was continuously synthesized to ensure the smooth transfer of electrons and protons inside and outside the thylakoid membrane in response to exposure to a low BPA concentration, as evidenced by the up-regulation of the 2-methyl-6-phytyl-1,4-hydroquinone methyltransferase (VTE3) gene, which is involved in the biosynthesis of plastoquinol. The calvin cycle fixes atmospheric CO_2 into a C3 metabolite through a reaction catalyzed by the ribulose-1,5-bisphosphate carboxylase/oxygenase (Rubisco), which serves as a precursor for all cellular constituents and most of the reduced carbon on Earth. Meanwhile, the activities of enzymes that generate the bicarbonate from CO_2 assimilation were enhanced, as evidenced by the up-regulated carbonic anhydrase (CA), which is responsible for converting the bicarbonate absorbed by algae into CO_2 for use by Rubisco (Yu et al., 2018). Therefore, the production of important metabolites, including 3-phosphoglycerate (3-PGA), glyceraldehyde 3-phosphate (GAP) and dihydroxyacetone phosphate (DHAP), during carbon fixation of algal cells will become increasingly favorable, creating a driving force to initiate the pathway of gluconeogenesis. Phosphoenolpyruvate carboxykinase (Ppc), involved in glycolysis/gluconeogenesis, citrate cycle, pyruvate metabolism and carbon fixation in photosynthetic organisms, was down-regulated triggered in the high BPA-treatment group. The Ppc gene is utilized in the C4 carbon-concentrating mechanism pathway (Hatch and Mau, 1977), where it slowly catalyzes the reaction of PEP and bicarbonate to produce oxaloacetate (Fig. 7).

The C4 carbon-concentrating mechanism pathways were noticeably activated by BPA stress. Glycolysis breaks down glucose to form pyruvate and acetyl-CoA. The expressions of glucokinase (MAE_18450), glucose-6-phosphate isomerase (MAE_16590), ATP-dependent phosphofructokinase (MAE_38160), fructose-bisphosphate aldolase, class II (MAE_32470), glyceraldeyde-3-phosphate dehydrogenase (MAE_25030), phosphoglycerate kinase (MAE_43670), 2,3-bisphosphoglycerate-independent phosphoglycerate mutase (MAE_32370), enolase (MAE_35090), pyruvate kinase (MAE_03940), and the E1 component beta subunit of subunit of pyruvate dehydrogenase (MAE_05620) and phosphoenolpyruvate carboxykinase (MAE_06160), were largely unchanged except for some downregulation. These genes produced pyruvate and acetyl-CoA, which fed into the tricarboxylic acid (TCA) cycle. Similarly, the genes in the TCA cycle were simultaneously down-regulated; the phosphoenolpyruvate carboxykinase (Ppc), which catalyzes the carboxylation of phosphoenolpyruvate (C3) to produce oxaloacetate (C4) and fixed CO_2, was used to replenish intermediates of the TCA cycle for amino acid biosynthesis or to shuttle CO_2 between the mesophyll and bundle sheath cells in C4 plants (nullvoklwaemmerqueogayyqukimsmykqmy). The down-regulated of Ppc would slow down the process of gluconeogenesis and TCA cycle. Meanwhile, the production of acetyl-CoA, a key precursor metabolite required for fatty acid synthesis and the TCA cycle, was also restrained through the down-regulation of genes involved in valine, leucine and isoleucine degradation. In summary, the glycolysis/gluconeogenesis, citrate cycle and pyruvate pathways were impaired, which subsequently adversely affected cell growth and metabolism. This metabolic mechanism may be the most important source of ROS. In addition, the process of oxidative phosphorylation was also inhibited by the down-regulated of heme O synthase (CyoE), which further inhibited the production of energy.

Additionally, the large subunits, 50S ribosomal protein L7/L12 (RplL) and 50S ribosomal protein L10 (RplJ), which are responsible for linking amino acids delivered by transfer RNA to form proteins, were up-regulated in the high BPA exposure group. This finding was consistent with the result that the differentially expressed genes in high BPA-treatment group were much more than that in low BPA-treatment group. Moreover, the expression level of iron(III) transport system substrate-binding protein (fbpA) that efficiently takes up iron together with the inner membrane transporter, FbpBC (Lu et al., 2019), was increased in low BPA treatment groups. Thus, the transport and metabolism of iron ions would be accelerated to generate a driving force to produce more energy and sustain cellular growth, which was consistent with the conclusion that less growth inhibition occurs in the low BPA treatment group (Fig. 1). However, after exposure to a high BPA concentration, the phospholipid/cholesterol/gamma-HCH transport system permease protein (MlaE) was down-regulated, which would inhibit phospholipid transport, and subsequently altered the spontaneous diffusion of the membrane to eventually caused membrane damage (Vance, 2015). The conserved adenosine triphosphate (ATP)-regulated initiator protein, DnaA, which was associated with two-component system and cell cycle- caulobacter, formed a complex with the origin, oriC, that mediated DNA strand separation and recruitment of replication machinery (Grimwade et al., 2018). The down-regulation of DnaA delayed the initiation of chromosome replication, resulting in lower than normal nucleotide levels, while insufficient nucleotides would slow fork movement directly and allow the machinery to encounter the DNA lesions caused by oxidative stress (Charbon et al., 2018; 2014), as evidenced by the inhibition of cellular growth and increased ROS values (Figs. 1 and 5a).

4. Conclusion

The study explored the regulatory mechanisms underlying the ecophysiological and molecular responses of cyanobacteria to endocrine-disrupting compounds. This study is the first to report the global transcriptional changes in cyanobacterial cells occurring in response to exposure to endocrine-disrupting compounds. M. aeruginosa exposed to high and low BPA caused 43 and 40 up-regulated genes respectively, which was primarily associated with folate biosynthesis, porphyrin and chlorophyll metabolism, ABC transporters, ribosome, photosynthesis and nitrogen metabolism. The 58 and 12 down-regulated genes were related to ubiquinone and other terpenoid-quinone biosynthesis, glycolysis/glyconeogenesis, citrate cycle, oxidative phosphorylation, carbon fixation in photosynthetic organisms and cell cycle-caulobacter, confirming that the genes with inhibited expression lead to an inhibition of cyanobacterial cell growth and slow energy metabolism and triggered oxidative damage, which was an adaptation mechanism of M. aeruginosa exposed to BPA.

CRediT author statement

This research was designed by Meng Yang and was funded from the program of Xiangrong Wang. Lab experiments were performed by Meng Yang. Data were analysed by Meng Yang. The paper was written by Meng Yang. Data interpretation and Draft corrections were involved in all the authors including Meng Yang, Zhengqiu Fan, Yujing Xie, Lei Fang, Xiangrong Wang, Yuan Yuan, Rongxi Li.

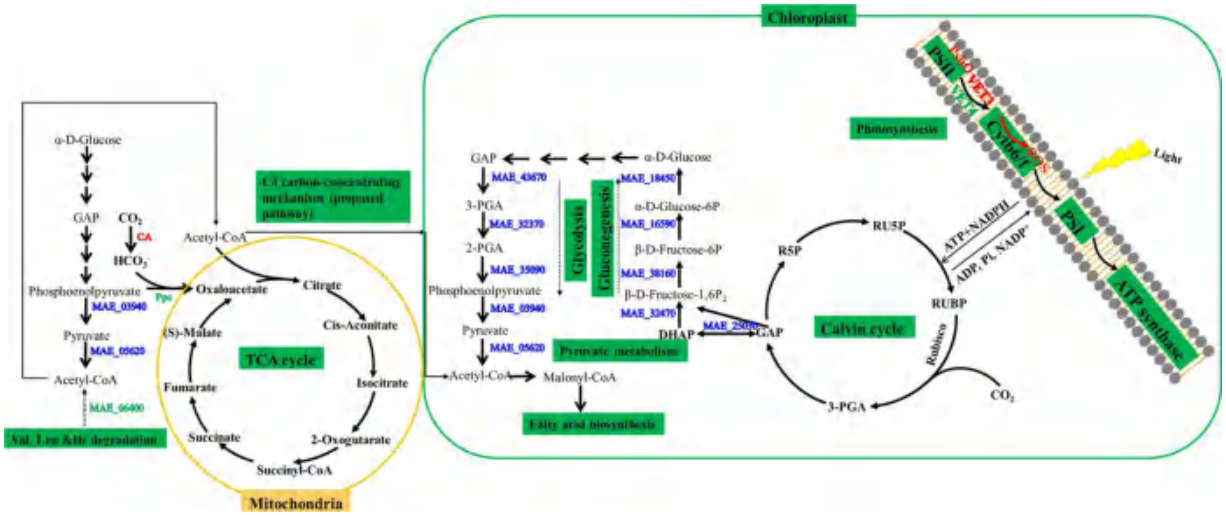

Fig. 7. Proposed schematized network of cellular pathways, enzymes and metabolites derived from transcriptome analyses in M. aeruginosa upon BPA stress. Arrows represent the biochemical pathways. Black font indicates that the metabolites. Bold gene names in red, green and blue indicate genes expression that was up- or down-regulated or stable expression in response to BPA treatment. Green boxes denote pathway names. Legend: Rubisco, ribulose-1,5-bisphosphate carboxylase/oxygenase; R5P, Ribose 5-phosphate; 3-PGA, 3-Phosphoglycerate; GAP, Glyceraldehyde 3-phosphate; RU5P, D-Ribulose 5-phosphate; RUBP, D-Ribulose 1,5-bisphosphate; DHAP, dihydroxyacetone phosphate; β-D-Fructose-1,6P2, beta-D-Fructose 1,6-bisphosphate; β-D-Fructose-6 P, beta-D-Fructose 6-phosphate; α-D-Glucose-6 P, alpha-D-Glucose 6-phosphate; 2-PGA, 2-Phospho-D-glycerate; CA, carbonic anhydrase. (For interpretation of the references to color in this figure legend, the reader is referred to the web version of this article.)

Declaration of Competing Interest

The authors declare that they have no known competing financial interests or personal relationships that could have appeared to influence the work reported in this paper.

Acknowledgement

The authors are sincerely thankful for the financial support from the China's Foundation of National Key Research and Development Plan Program (2016YFC0502700).

Appendix A. Supplementary data

Supplementary material related to this article can be found, in the online version, at doi:https://doi.org/10.1016/j.jhazmat.2020.122746.

References

Arnold, S.M., Clark, K.E., Staples, C.A., Klecka, G.M., Dimond, S.S., Caspers, N., Hentges, S.G., 2013. Relevance of drinking water as a source of human exposure to bisphenol A. J. Expo. Sci. Environ. Epidemiol. 23, 137–144.

Blokhina, O., Virolainen, E., Fagerstedt, K.V., 2003. Antioxidants, oxidative damage and oxygen deprivation stress: a review. Ann. Bot. 91, 179–194.

Boyer, G.L., 2007. The occurrence of cyanobacterial toxins in New York lakes: lessons from the MERHAB-Lower great lakes. Lake Reserv. Manag. 23, 153–160.

Charbon, G., Bjørn, L., Mendoza-Chamizo, B., Frimodt-Møller, J., Løbner-Olesen, A., 2014. Oxidative DNA damage is instrumental in hyperreplication stress-induced inviability of Escherichia coli. Nucleic Acids Res. 42, 13228–13241.

Charbon, G., Riber, L., Løbner-Olesen, A., 2018. Countermeasures to survive excessive chromosome replication in Escherichia coli. Curr. Genet. 64, 71–79.

Chen, J.Z., Dai, J., Zhang, H.Y., Wang, C.Y., Zhou, G.Q., Han, Z.P., Liu, Z.L., 2010. Bioaccumulation of microcystin and its oxidative stress in the apple (Malus pumila). Ecotoxicology 19, 796–803.

Corrales, J., Kristofco, L.A., Steele, W.B., Yates, B.S., Breed, C.S., Williams, E.S., Brooks, B.W., 2015. Global assessment of bisphenol A in the environment: review and analysis of its occurrence and bioaccumulation. DoseResponse 13.

Daly, R.I., Ho, L., Brookes, J.D., 2007. Effect of chlorination on Microcystis aeruginosa cell integrity and subsequent microcystin release and degradation. Environ. Sci. Technol. 41, 4447–4453.

Dodson, R.E., Nishioka, M., Standley, L.J., Perovich, L.J., Brody, J.G., Rudel, R.A., 2012. Endocrine disruptors and asthma-associated chemicals in consumer products. Environ. Health Perspect. 120, 935–943.

Fenichel, P., Chevalier, N., Brucker-Davis, F., 2013. Bisphenol A: an endocrine and metabolic disruptor. Ann. Endocrinol. 74, 211–220.

Fleisch, A.F., Sheffield, P.E., Chinn, C., Edelstein, B.L., Landrigan, P.J., 2010. Bisphenol A and related compounds in dental materials. Pediatrics 126, 760.

Foyer, C.H., LopezDelgado, H., Dat, J.F., Scott, I.M., 1997. Hydrogen peroxide- and glutathione-associated mechanisms of acclimatory stress tolerance and signalling. Physiol. Plant. 100, 241–254.

Gonçalves-Soares, D., Zanette, J., Yunes, J.S., Yepiz-Plascencia, G.M., Bainy, A.C.D., 2012. Expression and activity of glutathione S-transferases and catalase in the shrimp Litopenaeus vannamei inoculated with a toxic Microcystis aeruginosa strain. Mar. Environ. Res. 75, 54–61.

Grimwade, J.E., Rozgaja, T.A., Gupta, R., Dyson, K., Rao, P., Leonard, A.C., 2018. Origin recognition is the predominant role for DnaA-ATP in initiation of chromosome replication. Nucleic Acids Res. 46, 6140–6151.

Hatch, M.D., Mau, S.L., 1977. Properties of phosphoenolpyruvate carboxykinase operative in C4 pathway photosynthesis. Aust. J. Plant Physiol. 4, 207–216.

Hengstler, J.G., Foth, H., Gebel, T., Kramer, P.J., Lilienblum, W., Schweinfurth, H., Volkel, W., Wollin, K.M., Gundert-Remy, U., 2011. Critical evaluation of key evidence on the human health hazards of exposure to bisphenol A. Crit. Rev. Toxicol. 41, 263–291.

Huang, Y.Q., Wong, C.K.C., Zheng, J.S., Bouwman, H., Barra, R., Wahlstrom, B., Neretin, L., Wong, M.H., 2012. Bisphenol A (BPA) in China: a review of sources, environmental levels, and potential human health impacts. Environ. Int. 42, 91–99.

Jia, Y.L., Chen, Q.Q., Crawford, S.E., Song, L.R., Chen, W., Hammers-Wirtz, M., Strauss, T., Seiler, T.B., Schaffer, A., Hollert, H., 2019. Cyanobacterial blooms act as sink and source of endocrine disruptors in the third largest freshwater lake in China. Environ. Pollut. 245, 408–418.

Liu, Y., Guan, Y.T., Gao, B.Y., Yue, Q.Y., 2012. Antioxidant responses and degradation of two antibiotic contaminants in Microcystis aeruginosa. Ecotoxicol. Environ. Saf. 86, 23–30.

Liu, Y., Chen, S., Chen, X., Zhang, J., Gao, B., 2015. Interactions between Microcystis aeruginosa and coexisting amoxicillin contaminant at different phosphorus levels. J. Hazard. Mater. 297, 83–91.

Lu, T., Zhu, Y.C., Xu, J.H., Ke, M.J., Zhang, M., Tan, C.X., Fu, Z.W., Qian, H.F., 2018. Evaluation of the toxic response induced by azoxystrobin in the non-target green alga Chlorella pyrenoidosa. Environ. Pollut. 234, 379–388.

Lu, P., Moriwaki, Y., Zhang, M., Katayama, Y., Lu, Y., Okamoto, K., Terada, T., Shimizu, K., Wang, M., Kamiya, T., Fujiwara, T., Asakura, T., Suzuki, M., Yoshimura, E., Nagata, K., 2019. Functional characterisation of two ferric-ion coordination modes of TtFbpA, the periplasmic subunit of an ABC-type iron transporter from Thermus thermophilus HB8. Metallomics 11, 2078–2088.

Markou, G., Dao, L.H.T., Muylaert, K., Beardall, J., 2017. Influence of different degrees of N limitation on photosystem II performance and heterogeneity of Chlorella vulgaris. Algal Res.-Biomass Biofuels Bioprod. 26, 84–92.

Melcer, H., Klecka, G., 2011. Treatment of wastewaters containing bisphenol A: state of the science review. Water Environ. Res. 83, 650–666.

Michalowicz, J., 2014. Bisphenol A - sources, toxicity and biotransformation. Environ. Toxicol. Pharmacol. 37, 738–758.

Mittler, R., 2002. Oxidative stress, antioxidants and stress tolerance. Trends Plant Sci. 7, 405–410.

Ng, F.-L., Phang, S.-M., Periasamy, V., Yunus, K., Fisher, A.C., 2014. Evaluation of algal biofilms on indium tin oxide (ITO) for use in biophotovoltaic platforms based on photosynthetic performance. PLoS One 9.

Oukarroum, A., 2016. Change in photosystem II photochemistry during algal growth phases of Chlorella vulgaris and Scenedesmus obliquus. Curr. Microbiol. 72, 692–699.
Platt, T., Gallegos, C.L., Harrison, W.G., 1980. Photoinhibition of photosynthesis in natural assemblages of marine-phytoplankton. J. Mar. Res. 38, 687–701.
Qian, H.F., Chen, W., Sheng, G.D., Xu, X.Y., Liu, W.P., Fu, Z.W., 2008. Effects of glufosinate on antioxidant enzymes, subcellular structure, and gene expression in the unicellular green alga Chlorella vulgaris. Aquat. Toxicol. 88, 301–307.
Robinson, B.J., Hui, J.P.M., Soo, E.C., Hellou, J., 2009. Estrogenic compounds in seawater and sediment from Halifax Harbour, Nova Scotia, Canada. Environ. Toxicol. Chem. 28, 18–25.
Ronderos-Lara, J.G., Saldarriaga-Norena, H., Murillo-Tovar, M.A., Vergara-Sanchez, J., 2018. Optimization and application of a GC-MS method for the determination of endocrine disruptor compounds in natural water. Separations 5, 8.
Sajiki, J., Yonekubo, J., 2003. Leaching of bisphenol A (BPA) to seawater from polycarbonate plastic and its degradation by reactive oxygen species. Chemosphere 51, 55–62.
Sekizawa, J., 2008. Low-dose effects of bisphenol A: a serious threat to human health? J. Toxicol. Sci. 33, 389–403.
Shelby, M.D., 2008. NTP-CERHR Monograph on the Potential Human Reproductive and Developmental Effects of Bisphenol a, NTP CERHR MON. v, vii–ix, 1–64 passim.
Vance, J.E., 2015. Phospholipid synthesis and transport in mammalian cells. Traffic 16, 1–18.
von Caemmerer, S., Furbank, R.T., 2016. Strategies for improving C4 photosynthesis. Curr. Opin. Plant Biol. 31, 125–134.
Wu, X.H., Yan, Y.W., Wang, P.F., Ni, L.Q., Gao, J.Y., Dai, R.H., 2015. Effect of urea on growth and microcystins production of Microcystis aeruginosa. Bioresour. Technol. 181, 72–77.
Xiang, R., Shi, J.Q., Yu, Y., Zhang, H.B., Dong, C.C., Yang, Y.J., Wu, Z.X., 2018a. The effect of bisphenol A on growth, morphology, lipid peroxidation, antioxidant enzyme activity, and PS II in Cylindrospermopsis raciborskii and Scenedesmus quadricauda. Arch. Environ. Contam. Toxicol. 74, 515–526.
Xiang, R., Shi, J.Q., Zhang, H.B., Dong, C.C., Liu, L., Fu, J.K., He, X.Y., Yan, Y.J., Wu, Z.X., 2018b. Chlorophyll a fluorescence and transcriptome reveal the toxicological effects of bisphenol A on an invasive cyanobacterium, Cylindrospermopsis raciborskii. Aquat. Toxicol. 200, 188–196.
Xie, X.J., Zhou, Q.X., Lin, D.S., Guo, J.M., Bao, Y.Y., 2011. Toxic effect of tetracycline exposure on growth, antioxidative and genetic indices of wheat (Triticum aestivum L.). Environ. Sci. Pollut. Res. - Int. 18, 566–575.
Yang, F., Miao, L.F., 2010. Adaptive responses to progressive drought stress in two poplar species originating from different altitudes. Silva. Fenn. 44, 23–37.
Yang, M., Wang, X., 2019a. Interactions between Microcystis aeruginosa and coexisting bisphenol A at different phosphorus levels. Sci. Total Environ. 658, 439–448.
Yang, M., Wang, X.R., 2019b. Interactions between Microcystis aeruginosa and coexisting bisphenol A at different nitrogen levels. J. Hazard. Mater. 369, 132–141.
Ye, X.Y., Wong, L.Y., Kramer, J., Zhou, X.L., Jia, T., Calafat, A.M., 2015. Urinary concentrations of bisphenol A and three other bisphenols in convenience samples of US adults during 2000–2014. Environ. Sci. Technol. 49, 11834–11839.
Yu, H., Li, X., Duchoud, F., Chuang, D.S., Liao, J.C., 2018. Augmenting the Calvin–Benson–Bassham cycle by a synthetic malyl-CoA-glycerate carbon fixation pathway. Nat. Commun. 9, 2008.
Zhang, Q., Qu, Q., Lu, T., Ke, M., Zhu, Y., Zhang, M., Zhang, Z., Du, B., Pan, X., Sun, L., Qian, H., 2018. The combined toxicity effect of nanoplastics and glyphosate on Microcystis aeruginosa growth. Environ. Pollut. 243, 1106–1112.